GLOBAL SCALING OF OMA MODES SHAPES WITH THE OMAH METHOD

Brandt, A[1] and Berardengo, M[2] and Manzoni, S[3] and Vanali, M[2] and Cigada, A[3]

1 *University of Southern Denmark - Department of Technology and Innovation,*
Campusvej 55, DK-5230 Odense M, Denmark,
E-mail of the corresponding author: abra@iti.sdu.dk
2 *Università degli Studi di Parma - Department of Engineering and Architecture,*
Parco Area delle Scienze, 181/A - 43124 Parma, Italy
3 *Politecnico di Milano - Department of Mechanical Engineering,*
Via La Masa, 34 - 20156 Milan, Italy

ABSTRACT
Mode shapes obtained by operational modal analysis lack information about the modal scaling (or, modal mass). In many cases, this does not pose any limitation, but in certain cases, for example for some structural health monitoring methods, and computational model validation, a scaled modal model is important. We recently presented a new approach for scaling OMA modal models using harmonic excitation, called the OMAH method, and showed that this method is robust and reliable. The method relied, however, on excitation and response measurements in one measurement point for each mode. In the present paper, we extend the numerical processing of the measurements, taking many measurements across the structure into account for the scaling. This is analog to using so-called global parameter estimation in the classical experimental modal analysis (EMA) methods. We also propose an extension of the method to the case of multiple-reference analysis, which can be utilized when there is no single excitation point for which all modes have large mode shape coefficients.

KEYWORDS: operational modal analysis; mode scaling; modal mass

1. INTRODUCTION

Modal analysis is a tool for estimating modal parameters of systems/structures. The knowledge of eigenfrequencies and mode shapes is crucial for several different purposes, for example response estimation, model updating, and structural health monitoring. In many cases, the mode shape components must be properly scaled. This is one of the main problems of operational modal analysis (OMA), which in itself only provides unscaled mode shapes, because the loads acting on the structure are not measured.
Different methods were proposed in the past for scaling the mode shape components provided by OMA tests. Most of them require to repeat the OMA tests with different system configurations. This means to change, in a controlled way, the distribution/amount of the mass of the structure [1, 2, 3, 4, 5, 6, 7, 8, 9, 10, 11]. Other approaches couple known dynamic systems (e.g. tuned mass dampers, people) to the structure under investigation and this allows to estimate the modal mass and thus to scale the mode shapes [12, 13, 14]. Further approaches rely on the use of OMAX (operational modal analysis with exogenous inputs) tests. In this case the excitation to the structure is partly provided by natural environmental excitation (e.g. traffic, wind) and partly by actuators providing broadband excitation, which is thus measured [15, 16].
All the mentioned approaches require an accurate knowledge of the dynamics of additional systems, or ask for using potentially large actuators (on large structures) capable to produce different types of excitation signals (e.g. chirp, multi-harmonic), or, again, rely on relatively complicated experimental procedures (e.g. mass changes). Recently, the authors of the present paper proposed a new method to scale modes estimated by means of OMA employing mono-harmonic excitation [17, 18]. The method, which was proposed to be called OMAH, was shown to be robust and reliable. In [19], the estimation of the harmonic responses under various signal-to-noise ratios (SNR), using the three-parameter sine fit method, was investigated.
The present paper explains how to improve the accuracy of the scaling. This is accomplished by increasing the

number of degrees-of-freedom (DOF) in which the response to the mono-harmonic excitation is measured. Furthermore, an extension of the method is proposed for the case of multi-reference analysis.
The paper is structured as follows. Section 2 introduces the theory related to this work as well as the OMAH method proposed. Then, Section 3 explains how to improve accuracy by increasing the number of DOFs in which the response to the mono-harmonic excitation is measured. Here, numerical simulations will be employed to this purpose. Finally, Section 4 explains how to extend the method for multi-reference purposes. Again numerical simulations are used to prove the reliability of the approach.

2. THEORY

A scaled frequency response function of a structure can be formulated generally in receptance form (displacement over force) as:

$$H_{p,q}(\mathrm{j}\omega) = \sum_{r=1}^{N_m} \frac{\psi_r^p \psi_r^q Q_r}{(\mathrm{j}\omega - s_r)} + \frac{(\psi_r^p \psi_r^q Q_r)^*}{(\mathrm{j}\omega - s_r^*)} \tag{1}$$

where q is the DOF where excitation is provided and p is the DOF where the structural response is measured. Moreover, s_r the pole of mode r (* denotes complex conjugation). The expression of s_r is $-\zeta_r\omega_r + \omega_r\sqrt{1-\zeta_r^2}$, where ω_r and ζ_r are the eigenfrequency and non-dimensional damping ratio of mode r, respectively. Furthermore, ψ_r^p and ψ_r^q are the mode shape components of mode r at points p and q, respectively. N_m is the number of modes considered, j is the imaginary unit and, finally, Q_r is the modal scaling constant of mode r:

$$Q_r = \frac{1}{2\mathrm{j}m_r\omega_r\sqrt{1-\zeta_r^2}} \tag{2}$$

where m_r is the modal mass of mode r.
The expression provided in Equation (1) can many times alternatively be written (for example in the case of proportional damping) as:

$$H_{p,q}(\mathrm{j}\omega) = \sum_{r=1}^{N_m} \frac{\psi_r^q \psi_r^p}{m_r(\mathrm{j}\omega - s_r)(\mathrm{j}\omega - s_r^*)} \tag{3}$$

In OMA, the poles and the values of ψ_r^q and ψ_r^p are obtained by the parameter extraction, and, according to Equation (3), scaling the mode shape thus reduces to finding the modal mass m_r of the modes to be scaled.
The method proposed here is to achieve the modal scaling by applying a measured mono-harmonic force in one DOF, at (or close to) each natural frequency of the modes to be scaled. This single frequency measurement can then be used to obtain the scaling of the mode by assuming that the single mode is dominating at the excitation frequency considered, which will be equivalent to a single-degree-of-freedom (SDOF) approach [17]. However, also multi-degrees-of-freedom (MDOF) problems can be solved with an extension of the same approach [18].
The first part of the method proposed herein is thus to carry out an OMA, finding the s_r values and the corresponding unscaled mode shape components $\psi_r^{p_i}$, where p_i indicates generic points of the structure where its response has been measured during the OMA test. Then, the second part of the method consists of providing a known (i.e. measured) mono-harmonic excitation (at a frequency close to ω_r, indicated as ω_{ex}) to the structure in point q. It is essential that q is a point where $\psi_r^{p_i}$ has been found by means of OMA (i.e. q is a point where the structural vibration was acquired during the OMA test).
If we consider a SDOF approximation, the frequency response function (FRF) of Equation (3) at ω_{ex} can be approximated as:

$$H_{p,q}(\mathrm{j}\omega_{ex}) \simeq \frac{\psi_r^q \psi_r^p}{m_r(\mathrm{j}\omega_{ex} - s_r)(\mathrm{j}\omega_{ex} - s_r^*)} \tag{4}$$

If $H_{p,q}(\mathrm{j}\omega_{ex})$ is measured, the value of m_r can be estimated as:

$$m_r = \frac{\psi_r^q \psi_r^p}{H_{p,q}(\mathrm{j}\omega_{ex} - s_r)(\mathrm{j}\omega_{ex} - s_r^*)} \tag{5}$$

Of course, if higher accuracy is required, or if there are coupled modes so that several modes are contributing to the frequency response at frequency ω_{ex}, then $H_{p,q}(\mathrm{j}\omega_{ex})$ evaluated at several different frequencies ω_{ex} can be used; at least as many frequencies as the number of modes to be scaled. In fact, to obtain the best accuracy, at least two more frequencies than number of modes in the frequency range of interest should be excited, to allow for residual terms, accounting for the out-of-band modes, to be computed. The requested modal masses can then be

computed by using a standard least squares frequency domain method [20, 21]. Even in the case of using several frequencies of excitation, we propose using frequencies close to each eigenfrequency, as this will require lower force excitation, while still maintaining high response levels so that the SNR is kept as high as possible.

3. ACCURACY IMPROVEMENT BY INCREASING THE NUMBER OF DEGREES-OF-FREEDOM

The modal mass estimation requires to use the values of ψ_r^q and ψ_r^p. These values are affected by uncertainty and errors due to random errors in the correlation function estimates used for the OMA parameter extraction. Errors in the estimated values of ψ_r^q and ψ_r^p in turn affects the estimation of m_r and thus the reconstructed FRFs (i.e., FRFs built by using the estimated values of s_r, m_r, ψ_r^q and ψ_r^p).
Here, we propose to improve the accuracy of the mode shape scaling and thus of the reconstructed FRFs by increasing the number of DOFs used for the scaling. The driving idea is to measure the structural response in more than one DOF (i.e., $p_1, p_2, ..., p_m$) when applying the mono-harmonic excitation. All these DOFs must correspond to DOFs where the structural response was measured also in the OMA tests.
The following matrix equation can be written:

$$\mathbf{H} = \mathbf{A}\frac{1}{m_r} \tag{6}$$

where

$$\mathbf{H} = \begin{bmatrix} H_{p_1,q}(\mathrm{j}\omega_{ex}) \\ H_{p_2,q}(\mathrm{j}\omega_{ex}) \\ \vdots \\ H_{p_m,q}(\mathrm{j}\omega_{ex}) \end{bmatrix} \tag{7}$$

and

$$\mathbf{A} = \begin{bmatrix} \frac{\psi_r^{p_1}\psi_r^q}{(\mathrm{j}\omega_{ex}-s_r)(\mathrm{j}\omega_{ex}-s_r^*)} \\ \frac{\psi_r^{p_2}\psi_r^q}{(\mathrm{j}\omega_{ex}-s_r)(\mathrm{j}\omega_{ex}-s_r^*)} \\ \vdots \\ \frac{\psi_r^{p_m}\psi_r^q}{(\mathrm{j}\omega_{ex}-s_r)(\mathrm{j}\omega_{ex}-s_r^*)} \end{bmatrix} \tag{8}$$

Solving Equation (6) by means of Least Squares or pseudo-inversion allows to estimate m_r. The use of many DOFs together for finding m_r is expected to improve the accuracy of the estimation because it uses more statistically uncorrelated data, as the errors in each mode shape coefficient and frequency response estimate are uncorrelated. The accuracy improvement was investigated by means of numerical simulations. Two different cases are discussed in subsections 3.1 and 3.2.

3.1. First numerical test

In the first simulation case we assume a SDOF system with undamped natural frequency $f_r = 5$ Hz, and relative damping $\zeta = 0.005$, i.e. 0.5 %. Also, we assume the mode shapes are scaled so that the modal mass is unity, i.e. $m_r = 1$. In the simulations we assume the OMA test was carried out by measuring the structural response in 7 DOFs (i.e., $p_1, p_2, ..., p_7$), due to harmonic excitation in one DOF, and we assume the poles to be correctly estimated. All the 7 DOFs are assumed to have the same value of the eigenvector component: $\psi_r^{p_1} = \psi_r^{p_2} = ... = \psi_r^{p_7} = Z$=0.02. However, to simulate errors in the estimates, the values of $\psi_r^{p_i}$ used, are set to $Z + e_i$, where e_i is a number randomly extracted from a uniform distribution with bounds equal to $\pm Z/10$. The erroneous values of the mode shape coefficients are denoted $\tilde{\psi}_r^{p_i}$.
An estimate of the modal mass was then computed using the mode shapes coefficients with random errors in Equation (8), and using the correct frequency responses in Equation (7), and solving Equation (6). Once the modal mass, m_r, was estimated, the FRF between a force applied in DOF p_1 and the displacement measured in DOF p_i was reconstructed by means of the following formulation:

$$\tilde{H}_{p_i,p_1}(\mathrm{j}\omega) \simeq \frac{\tilde{\psi}_r^{p_i}\tilde{\psi}_r^{p_1}}{m_r(\mathrm{j}\omega - s_r)(\mathrm{j}\omega - s_r^*)} \tag{9}$$

Using the reconstructed FRFs of Equation (9), the corresponding peak amplitude $\tilde{M}_i = \max\left[\left|\tilde{H}_{p_i,p_1}(\mathrm{j}\omega)\right|\right]$ was found. The value of $\tilde{M}_i$ was then compared to its true value,M_i, and the relative error defined by:

$$E_i[\%] = \frac{\tilde{M}_i - M_i}{M_i} 100 \tag{10}$$

was used for comparison. The whole procedure was repeated 1000 times by means of a Monte Carlo simulation. This allowed to build a statistical population of E_i values and to estimate the corresponding mean value $\bar{E}_i$ and standard deviation σ_i.

First, the OMAH mode shape scaling was carried out using only DOF p_1, the assumed excitation DOF. Subsequently, the number of DOFs used for the scaling was increased: employing p_1 and p_2 at first, then using p_1, p_2 and p_3, and so on, until all the 7 DOFs were used together to solve Equation (6). The index E_i was estimated in all these cases, as well as the mean $\bar{E}_i$ and the standard deviation σ_i (1000 simulations were carried out for each case). It should be noticed that the simulation was designed such that the extracted values of errors e_i used in a given run of the Monte Carlo simulation when using 1 DOF for scaling were exactly the same as those used in the same run of the Monte Carlo simulations when using 2 DOFs for scaling, 3 DOFs, and so on.

Figures 1 and 2 show the results in terms of $\bar{E}_i$ and σ_i, respectively, for the different numbers of DOFs used to solve Equation (6). As for the the mean $\bar{E}_i$, the values are close to zero even for a single DOF used for scaling, and there is no apparent improvement as a function of the number of DOFs used for scaling. However, it is evident that, when the number of DOFs is increased, the overall accuracy of the reconstructed FRFs improve. This is evidenced by the standard deviations shown in Figure 2, which (overall) decrease when using more than one DOF for scaling, except for the case of the actual DOF used for the scaling, when using only a single DOF. It is also worth noting that *all* values of σ_i decrease when the number of DOFs used for scaling is increased, also the standard deviations for the DOFs not used for scaling.

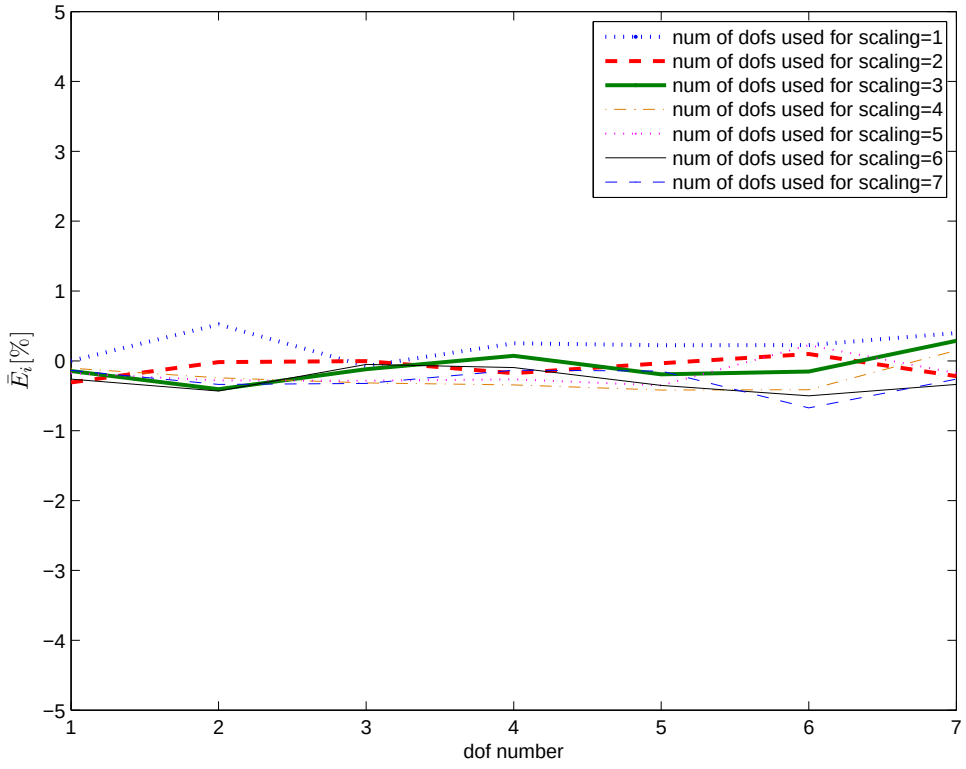

Figure 1 – Values of $\bar{E}_i$ for each DOF, and for different numbers of DOFs used for scaling

3.2. Second numerical test

The second type of numerical test is similar to the first one (see Section 3.1), except for the number of DOFs taken into account (18 in this case) and for the values of $\psi_r^{p_i}$ (this time not all the eigenvector components have the same nominal value). In this case, the first Monte Carlo simulation was carried out using 3 DOFs for scaling: $\psi_r^{p_1} = Z$=0.02, $\psi_r^{p_2} = Z/2$ and $\psi_r^{p_3} = Z/10$. Then, to simulate errors in their estimates, the value $\psi_r^{p_i}$ used were

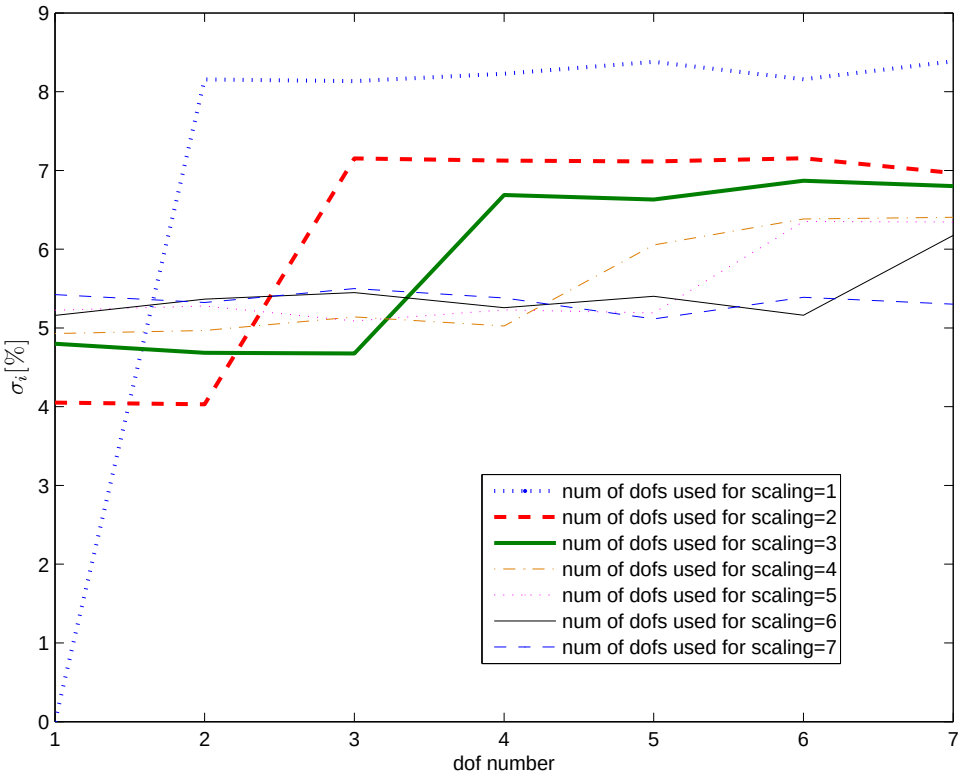

Figure 2 – Values of σ_i for each DOF, and for different numbers of DOFs used for scaling

equal to $\tilde{\psi}_r^{p_i} = \psi_r^{p_i} + e_i$, where e_i was a number randomly extracted from a uniform distribution with bounds equal to $\pm Z/10$. This means that a high error is expected on the lowest mode components. The results are still expressed in terms of $\bar{E}_i$ and σ_i for the 18 DOFs (the values of the different $\psi_r^{p_i}$ components are provided in Table 1). Excitation was applied in DOF p_1 and the Monte Carlo simulation was still made up by 1000 runs.

Table 1 – Values of $\psi_r^{p_i}$ for the different DOFs

DOFs with $\psi_r^{p_i} = Z$	DOFs with $\psi_r^{p_i} = Z/2$	DOFs with $\psi_r^{p_i} = Z/10$
1, 4, 7, 10, 13, 16	2, 5, 8, 11, 14, 17	3, 6, 9, 12, 15, 18

Then, the number of DOFs used for scaling were increased in steps of 3 DOFs; the first six DOFs, then the first nine and so on. Among the 3 DOFs added each time, one has always a nominal value equal to Z, one equal to $Z/2$ and one equal to $Z/10$ (see Table 1). Therefore, this allowed to simulate cases where also low-value mode components are used for scaling. The increase of the number of DOFs used does not provide significant changes in terms of $\bar{E}_i$, which is always in the order of a few percent (see Figure 3). However, the increase of the number of DOFs employed for scaling is advantageous; indeed, the largest values of σ_i for the points with $\psi_r^{p_i} = Z$ and $Z/2$ are reduced, as pointed out in Figures 4a and b, showing behaviors close to those already evidenced in Figure 2.
The improvements achievable by increasing the number of DOFs used for scaling are not only due to the increase of the number of scalar equations used for scaling. As an example, if the number of scalar equations is increased by adding mono-harmonic tests at different excitation frequencies [18] and always the same DOF is used for scaling, an improvement will be achieved just on the DOF used for scaling, but not on the other DOFs. Conversely, the accuracy of the estimate on all the DOFs is improved by increasing the number of DOFs over which scaling is performed.

4. MULTI-REFERENCE APPROACH

Using a single DOF for scaling the mode shapes, will only be successful in cases where a DOF for application of the force, that is not on a node line for any of the modes to be scaled, can be found. Preferably, for each mode to be scaled, the DOF where the force is applied should be a DOF where the mode in question has a large mode shape

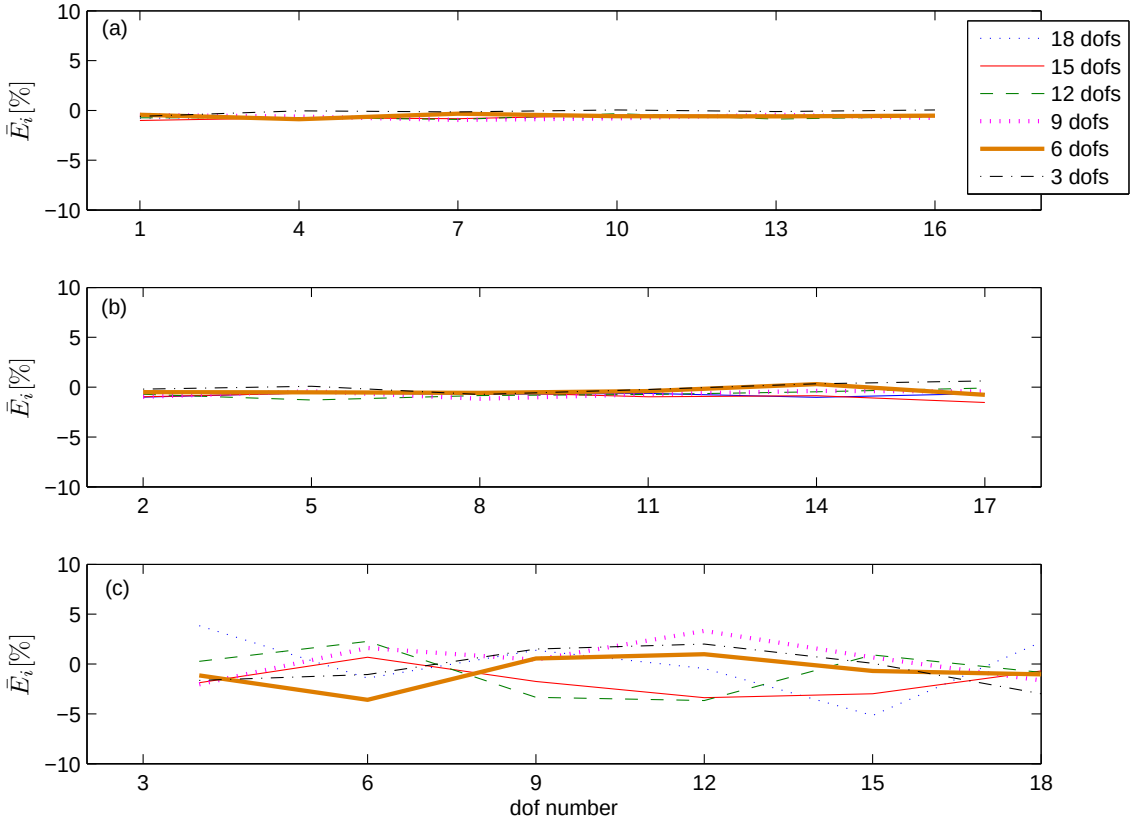

Figure 3 – Values of $\bar{E}_i$ for different numbers of DOFs used for scaling (see the figure legend); (a) DOFs with $\psi_r^{p_i} = Z$, (b) DOFs with $\psi_r^{p_i} = Z/2$ and (c) DOFs with $\psi_r^{p_i} = Z/10$

coefficient. In cases where a single point with large mode shape coefficients for all modes is not available, harmonic excitation can be applied in several DOFs, one at the time, which we refer to as multiple reference excitation.

A special case where multiple references may need to be used are systems with axis-symmetry, as twin (repeated) modes appear on such structures, nominally at the same frequency, but with mode shapes rotated with respect to each other, so that the maximum of one of the twin modes lies on the nodal line of the other mode. As an example, if we consider a disc, twin modes like those in Figure 5 will be encountered. In theory, the two twin modes at a particular frequency for the circular disc are undetermined in space, i.e. any linear combination of the two orthogonal modes are modes of the plate. This will mean that applying only one shaker will excite one of the modes, whereas the other mode will not be excited at all. In cases where a non-perfect axis-symmetry exists, which is a common case in practical applications, the two modes will be fixed in space. It may still lead to better mode shape scaling using more than one excitation DOF for such cases, as it is hard to find a DOF where both mode shapes have significant mode shape coefficients.

The usual practice in experimental modal analysis (EMA) with modes like those in Figure 5 is to use a multiple–reference approach. The optimal choice of the reference DOFs in EMA would be to use DOF 1 as reference for identifying mode 1A and DOF 3 for mode 1B, allowing to have response measurements with perfectly decoupled modes. However, any other choice of the reference DOFs is valid, except for two DOFs on a nodal line of the same mode, assuming one would use a multiple-reference parameter estimation method. Something similar can be done with the method presented here for scaling the modal model found with OMA. For the reader used to EMA considerations, it may, however, be worth pointing out that the OMA scaling case is somewhat different. Since the poles and mode shapes are estimated in the OMA parameter estimation, it will be the references used for the OMA test that determine how well the mode shapes of closely coupled modes can be separated. This should rarely pose any problems because multiple references should routinely be used for OMA. The OMAH mode shape scaling method thus only relies on the fact that excitation points are chosen, where each mode to be scaled has a significant mode shape coefficient.

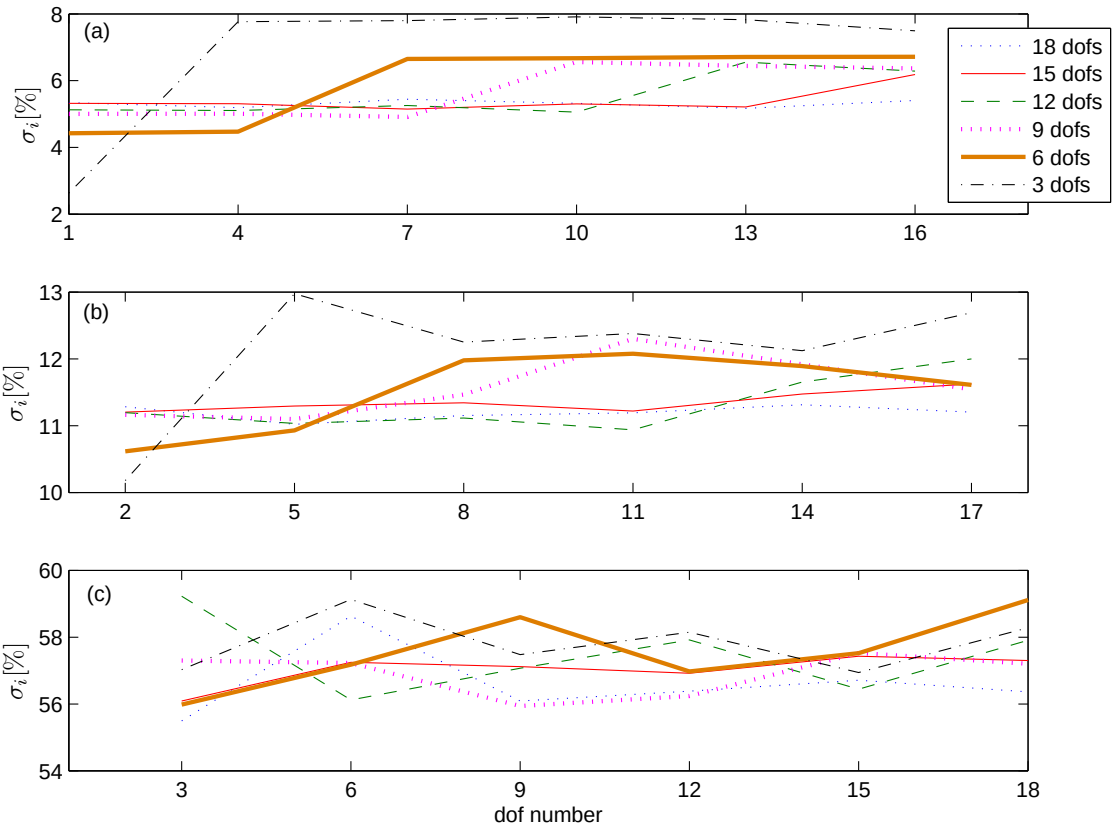

Figure 4 – Values of σ_i for different numbers of DOFs used for scaling (see the figure legend); (a) DOFs with $\psi_r^{p_i} = Z$, (b) DOFs with $\psi_r^{p_i} = Z/2$, and (c) DOFs with $\psi_r^{p_i} = Z/10$

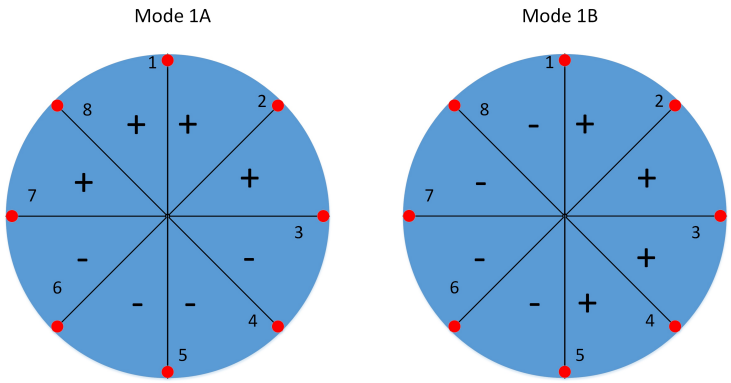

Figure 5 – Twin modes for a disc. The red circles are assumed accelerometer positions measuring the out-of-plane motion. The +/- signs indicate the out-of-plane motion of each portion of the disc.

4.1. Multiple-reference theory

To illustrate using multiple references (excitation DOFs) to scale the mode shapes of an OMA test, we will use the circular disc in Figure 5, supposing to have a non-perfect axis-symmetry so that modes 1A and 1B have slightly different natural frequencies. However, in practice, the same problem of scaling the mode shapes using a single DOF will occur for any structure where any choice of a single DOF for excitation, will be in a DOF where at least one mode has a small mode shape coefficient. This is the case for simply supported beam–like structures, for example, such as bridges.

The general (single reference, or excitation point) MDOF formulation for OMAH [18], assuming that we have N modes in the frequency range of interest, is based on a number of estimates, at different frequencies, of the frequency response between response DOF p and excitation DOF q:

$$\mathbf{H}_m = \begin{bmatrix} H_{p,q}(j\omega_{ex,1}) \\ \vdots \\ H_{p,q}(j\omega_{ex,k}) \end{bmatrix} \tag{11}$$

measured at k frequencies $\omega_{ex,1}, \omega_{ex,2}, ..., \omega_{ex,k}$. To find a solution for the multiple-reference case, we assume we do not have any effects of out-of-band modes. This should, however, in most OMA cases not be any important limitation, since we will usually start by the first mode, so there will be no effect of lower modes. For the higher modes, there will be some contribution, but if we excite the structure near its eigenfrequencies, the effect of the out-of-band modes should be negligible in most cases. With these assumptions we define the vector $\mathbf{x_m}$ with the unknown modal masses by:

$$\mathbf{x}_m = \begin{bmatrix} \frac{1}{m_1} \\ \vdots \\ \frac{1}{m_N} \end{bmatrix} \tag{12}$$

Next, we define a matrix $\mathbf{A_m}$ using the known mode shape coefficients and poles:

$$\mathbf{A}_m = \begin{bmatrix} \frac{\psi_1^p \psi_1^q}{(\mathrm{j}\omega_{ex,1} - s_1)(\mathrm{j}\omega_{ex,1} - s_1^*)} & \cdots & \frac{\psi_N^p \psi_N^q}{(\mathrm{j}\omega_{ex,1} - s_N)(j\omega_{ex,1} - s_N^*)} \\ \vdots & \vdots & \\ \frac{\psi_1^p \psi_1^q}{(\mathrm{j}\omega_{ex,k} - s_1)(\mathrm{j}\omega_{ex,k} - s_1^*)} & \cdots & \frac{\psi_N^p \psi_N^q}{(\mathrm{j}\omega_{ex,k} - s_N)(j\omega_{ex,k} - s_N^*)} \end{bmatrix} \tag{13}$$

which allows us to formulate the matrix equation:

$$\mathbf{H}_m = \mathbf{A}_m \mathbf{x}_m \tag{14}$$

Based on the development in Section 3 , in cases where all modes are well excited by the excitation in DOF q, and where $k \geq N$ (more frequencies than unscaled modes), Equation (14) can be solved by a least squares or Moore–Penrose pseudo inverse solution. However, in the case at hand here, where one or more of the mode shape coefficients ψ_r^q are zero, the matrix A_m will be singular, because a whole column will contain zeros. In order to cope with this case, we extend the vector H_m to include l frequencies with excitation in another DOF, s:

$$\mathbf{H}'_m = \begin{bmatrix} H_{p,q}(j\omega_{ex,1}) \\ \vdots \\ H_{p,q}(j\omega_{ex,k}) \\ H_{p,s}(j\omega_{ex,1}) \\ \vdots \\ H_{p,s}(j\omega_{ex,l}) \end{bmatrix} \tag{15}$$

and then extend matrix A_m with a number of rows for this second excitation DOF, which gives us:

$$\mathbf{A}'_m = \begin{bmatrix} \frac{\psi_1^p \psi_1^q}{(\mathrm{j}\omega_{ex,1}-s_1)(\mathrm{j}\omega_{ex,1}-s_1^*)} & \cdots & \frac{\psi_N^p \psi_N^q}{(\mathrm{j}\omega_{ex,1}-s_N)(j\omega_{ex,1}-s_N^*)} \\ \vdots & \vdots & \\ \frac{\psi_1^p \psi_1^q}{(\mathrm{j}\omega_{ex,k}-s_1)(\mathrm{j}\omega_{ex,k}-s_1^*)} & \cdots & \frac{\psi_N^p \psi_N^q}{(\mathrm{j}\omega_{ex,k}-s_N)(j\omega_{ex,k}-s_N^*)} \\ \frac{\psi_1^p \psi_1^s}{(\mathrm{j}\omega_{ex,1}-s_1)(\mathrm{j}\omega_{ex,1}-s_1^*)} & \cdots & \frac{\psi_N^p \psi_N^s}{(\mathrm{j}\omega_{ex,1}-s_N)(j\omega_{ex,1}-s_N^*)} \\ \vdots & \vdots & \\ \frac{\psi_1^p \psi_1^s}{(\mathrm{j}\omega_{ex,l}-s_1)(\mathrm{j}\omega_{ex,l}-s_1^*)} & \cdots & \frac{\psi_N^p \psi_N^s}{(\mathrm{j}\omega_{ex,l}-s_N)(j\omega_{ex,l}-s_N^*)} \\ \vdots & \vdots & \end{bmatrix} \tag{16}$$

Using these changes we define a new matrix equation:

$$\mathbf{H}'_m = \mathbf{A}'_m \mathbf{x}_m \tag{17}$$

which can now be solved for $\mathbf{x}_m$, because the extended matrix $\mathbf{A}'_m$ is not singular, since it now includes nonzero values in the column where $\psi_r^q = 0$, because there ψ_r^s is assumed to not equal zero. Note that it might be that the extended matrix $\mathbf{A}'_m$ also includes zeros in the column where the mode shape coefficient $\psi_r^s = 0$, because DOF s is on a node line for some mode. But since in that column, presumably, $\psi_r^q \neq 0$ the matrix is nonsingular (and thus invertable).

It should be noted, that the extension of using more than one response point, p, discussed in Section 3, means repeating the column vector $\mathbf{H}'_m$ and the matrix $\mathbf{A}'_m$ with additional rows in Equation (16) for each new response point p_i. This should usually be used, because it reduces the variance of the modal mass estimates, as was shown in Section 3.

Some important facts with the formulation suggested here should be mentioned. First, that the number of frequencies used for excitation in DOFs q and s, respectively, in the rows of Equation (15) and Equation (17), may well be different frequencies (although we did not specify that in the equations). This may be important, since when exciting the structure with a harmonic force in a new DOF, s, it may not be possible to excite with exactly the same frequency as was used when exciting DOF q because of inaccuracies in the signal generation system, for example. In addition, when exciting the second excitation DOF, it is not necessary to excite using as many frequencies as those used in the first excitation DOF, q, i.e. $k \neq l$. Indeed, only a single excitation frequency may be sufficient in DOF s, if there is only one mode for which DOF q is on a node line. The important point is, that all modes must, as a minimum, be excited at least once by either the excitation in DOF q or in DOF s. This will ensure that the matrix $\mathbf{A}'_m$ is non-singular and can thus be inverted. Finally, obviously more excitation DOFs could be added to the system in Equation 17 if necessary.

4.2. Numerical test

In order to investigate if this multiple-reference approach to mono-harmonic scaling is robust to errors in the positions of the forcing DOFs, the following simulations were performed. Referring to Figure 5, the optimal solution is to force mode 1A in DOF 1 and mode 1B in DOF 3. In such a way, only one mode provides a response to the excitation, while the other does not respond because it is forced at a node. However, in practical applications, deviations of the position of the excitation/measurement DOFs from their optimal locations can occur. This deviation is described by using the angle φ (see Figure 6). The numerical test carried out to investigate the effect of non-null values of φ is described in Section 4.2.

The simulations are aimed at answering the following questions. We assume that the values of the modal parameters extracted with OMA are affected by a random error (as usual in practical applications). Furthermore, let us suppose we use, in the mono-harmonic tests, reference DOFs which do not fully decouple the two modes (e.g. DOFs 1 and 2). When we apply this mono-harmonic scaling for the modal mass estimation, we will have FRFs with modes not decoupled where the modal parameters of both the modes contribute. Does this cause a combination of both errors (the ones related to the modal parameters of the first mode and the ones on the modal parameters related to the second mode) and thus a worsening of the results of the minimization carried out to find the modal masses? Does this worsen the modal mass estimation with respect to the case where a single DOF contributes to each FRF (i.e. when we use DOFs 1 and 3 as references and we decouple the modes) and thus just the errors on that mode must be accounted for?

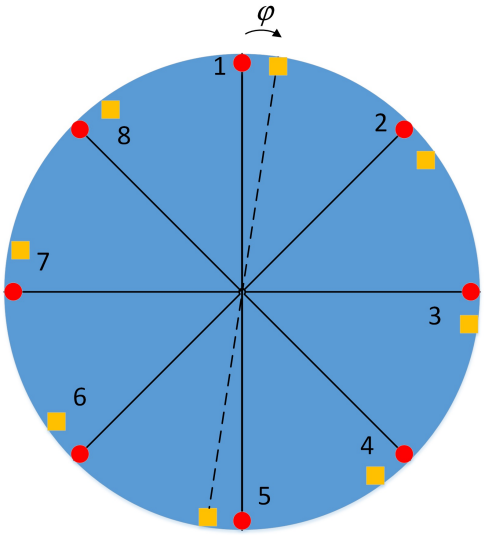

Figure 6 – Deviation from the optimal positions for the DOFs where structural response is measured/excitation is provided (from red circles to orange squares). This deviation is described by the angle φ.

Table 2 – Values of the standard deviations of the Gaussian distributions from which the error was extracted for $\psi_r^{p_i}$, ω_r and ζ_r.

$\psi_r^{p_i}$	ω_r	ζ_r
0.05	0.002	0.1

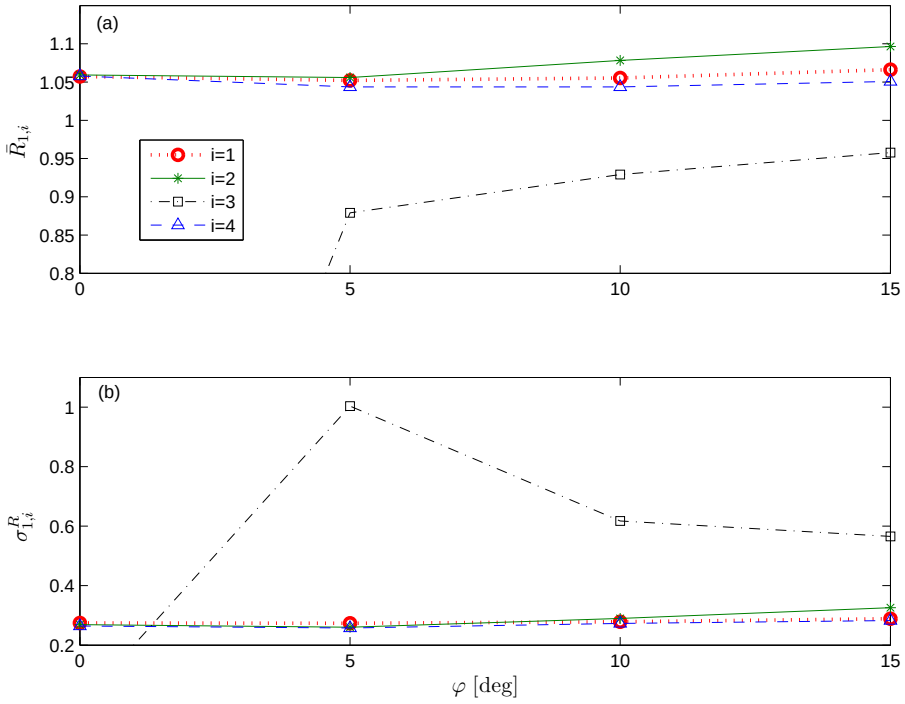

Figure 7 – Values of $\bar{R}_{1,i}$ (a) and $\sigma^R_{1,i}$ (b) as function of the angle φ.

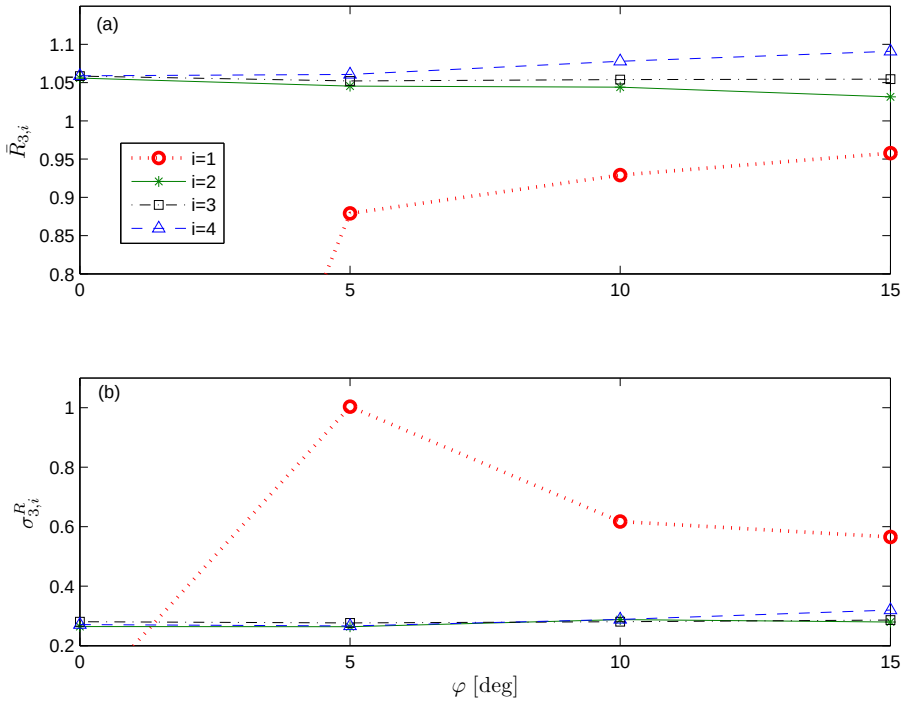

Figure 8 – Values of $\bar{R}_{3,i}$ (a) and $\sigma^R_{3,i}$ (b) as function of the angle φ.

Modes 1A and 1B (see Figure 5) are herein described by a cosine function and a sine function, respectively, with unitary amplitude:

$$\psi_{1A}(\alpha) = cos(2\pi\alpha), \qquad \psi_{1B}(\alpha) = sin(2\pi\alpha) \tag{18}$$

where α is a real number and $\alpha \in [0,1)$. $\alpha = 0$ corresponds to DOF 1 in Figure 5. The eight eigenvector components related to the DOFs where accelerometers are (supposed to be) placed (see Figures 5 and 6) are described by:

$$\psi^{p_i}_{1A} = cos((\pi/4)(i-1)+\varphi), \qquad \psi^{p_i}_{1B} = sin((\pi/4)(i-1)+\varphi) \tag{19}$$

The modal mass value are assumed to be unity.
Next, mode 1A was associated to an eigenfrequency value equal to 5.00 Hz and 1B to 5.02 Hz; the non-dimensional damping ratio was set to 0.5% for both modes. The reference DOFs for the mono-harmonic excitation were assumed to be DOFs 1 and 3.
Then, Equation (17) was solved using $\omega_{ex,1} = 2\pi 5.00$ rad/s and $\omega_{ex,2} = 2\pi 5.02$ rad/s, assuming to perfectly know the poles of the system and eigenvector components and that φ was null. The modal mass values obtained by the Least Square problem were used to reconstruct the peak amplitudes of the FRFs between a force in DOF 1 and responses in DOFs 1 to 8. Then, the same was carried out for a force applied in DOF 3. The errors between the reconstructed peaks and the real peaks were always negligible. This occurred also for the other tested values of φ: 0 rad, $5\pi/180$ rad (i.e., 5 deg), $10\pi/180$ rad (i.e., 10 deg) and $45\pi/180$ rad (i.e., 45 deg). This means that the minimization is not affected by deviations from the optimal multiple-reference configuration ($\varphi = 0$ rad).
The same simulations were then carried out supposing to have uncertainty on pole and eigenvector component values, as in real cases where the estimation by means of OMA cannot provide the actual values and errors are obviously unavoidable. Therefore, before solving Equation (17), an error was imposed by Gaussian distributions (with zero mean value) for each of the parameters (i.e., poles and eigenvector components). The standard deviations of the Gaussian distributions used for the various parameters are gathered in Table 2.
Since this procedure required some statistical extractions, it was repeated 2000 times to build a statistical population of errors for each tested φ value: 0 rad, $5\pi/180$ rad (i.e., 5 deg), $10\pi/180$ rad (i.e., 10 deg) and $15\pi/180$ rad (i.e., 15 deg).

These statistical populations are described in terms of mean value and standard deviation of the index $R_{q,i}$:

$$R_{q,i} = \frac{M_{q,i}}{\tilde{M}_{q,i}} 100 \tag{20}$$

where $M_{q,i}$ is the real peak amplitude for the FRF between a force in DOF q and a response measured at DOF p_i; $\tilde{M}_{q,i}$ is the reconstructed peak amplitude for the FRF between a force in DOF q and a response measured at DOF p_i.

Figures 7 and 8 show the values of the mean value ($\bar{R}_{q,i}$) and standard deviation ($\sigma^R_{q,i}$) of the index $R_{q,i}$, respectively. It is evident that again there are no clear trends due to the value of φ, as in the case of no errors on the modal parameters estimated by means of OMA; actually, a slight deterioration of the results can be observed for some DOFs and φ equal to 15 deg, but, as said, it is slight.

It is noticed that the points of Figures 7 and 8 which are at zero (these points are not displayed in the figures: they are related to the dashed-dotted lines in Figure 7 and to the dotted lines in Figure 8 at $\varphi = 0$) are meaningless. Indeed, their null value completely depends on the value of $M_{q,i}$ and are not related to the value of $\tilde{M}_{q,i}$ (see Equation (20)).

The above results mean that the multiple-reference procedure to compute the modal masses is robust to DOF positions where excitation is provided and response is measured and no significant increase in errors is expected from the scaling procedure.

Attention must be paid to decrease the errors associated with the modal parameters (poles and eigenvector components) estimated by means of OMA; indeed, high errors obviously worsen the results of the scaling procedure. However, the mono-harmonic tests and the subsequent minimization carried out for scaling the modes do not seem to introduce additional errors on the final results.

5. CONCLUSIONS

This paper has presented an extension of a recently presented innovative method for scaling mode shapes estimated by means of operational modal analysis, the OMAH method. This method is based on exciting the test structure by mono-harmonic forces at a number of frequencies and in at least two different DOFs. In the present paper, two particular points are addressed: the increase in accuracy of the scaling procedure by increasing the number of degrees-of-freedom employed for finding the modal masses, and the extension of the method to the multiple-reference case for cases where one excitation point with high mode shape coefficients cannot be found.

Numerical simulations showed that increasing the number of response DOFs used for the modal scaling, reduced the variance in the modal mass estimates. We refer to this as *global scaling*, similarly with terminology used in experimental modal analysis (EMA). It should always be recommended to use more response DOFs than using only the frequency response in the excitation point for the scaling. This can readily be done by using the same setup as the one used for the OMA data acquisition, for example.

When applying the OMAH method, for each mode to be scaled, the structure should preferably be excited in a DOF where the mode to be scaled has a large mode shape coefficient. On many structures, one DOF cannot be found which satisfies this criterion for all modes. Thus more than one DOF may have to be chosen for excitation. Furthermore, on structures where two or more modes are closely coupled, a multiple degree of freedom method must be used for successful mode scaling, where several frequencies are measured, and several modes are scaled simultaneously. A multiple-reference, global, MDOF method was developed in the present paper, and simulations showed that it successfully scaled the modes of a circular symmetric disc.

REFERENCES

[1] PARLOO, E., VERBOVEN, P., GUILLAUME, P., VAN OVERMEIRE, M., "Sensitivity-Based Operational Mode Shape Normalisation", Mechanical Systems and Signal Processing, 16(5), 2002, pp. 757–767.

[2] Parloo, E., Cauberghe, B., Benedettini, F., Alaggio, R., Guillaume, P., "Sensitivity-based operational mode shape normalisation: Application to a bridge", Mechanical Systems and Signal Processing, 19(1), 2005, pp. 43–55.

[3] Bernal, D., "Modal Scaling from Known Mass Perturbations", Journal of engineering mechanics, 130(9), 2004, pp. 1083–1088.

[4] Bernal, D., "A receptance based formulation for modal scaling using mass perturbations", Mechanical Systems and Signal Processing, 25(2), 2011, pp. 621–629.

[5] Coppotelli, G., “On the estimate of the FRFs from operational data”, Mechanical Systems and Signal Processing, 23(2), 2009, pp. 288–299.

[6] Lopez-Aenlle, M., Fernandez, P., Brincker, R., Fernandez-Canteli, A., “Scaling-factor estimation using an optimized mass-change strategy”, Mechanical Systems and Signal Processing, 24(5), 2010, pp. 1260–1273.

[7] Lopez-Aenlle, M., Brincker, R., Pelayo, F., Canteli, A.F., “On exact and approximated formulations for scaling-mode shapes in operational modal analysis by mass and stiffness change”, Journal of Sound and Vibration, 331(3), 2012, pp. 622–637.

[8] Brincker, R., Andersen, P., “A Way of Getting Scaled Mode Shapes in Output Only Modal Testing”, Proceedings of International Modal Analysis Conference (IMAC) - 3-6 February 2003, Orlando (USA), 2003.

[9] Brincker, R., Rodrigues, J., Andersen, P., “Scaling the Mode Shapes of a Building Model by Mass Changes”, Proceedings of International Modal Analysis Conference (IMAC) - 26-29 January 2004, Dearborn (USA), 2004.

[10] Aenlle, L., Brincker, R., Canteli, A.F., “Some Methods to Determine Scaled Mode Shapes in Natural Input Modal Analysis”, Proceedings of International Modal Analysis Conference (IMAC) - January 31-February 3 2005, Orlando (USA), 2005, pp. 1–11.

[11] Fernández, P., Lopez-Aenlle, M., Garcia, L., Brincker, R., “Scaling Factor Estimation Using an Optimized Mass Change Strategy . Part 1 : Theory”, Proceedings of International operational modal analysis conference (IOMAC) - April 30-May 2 2007, Copenhagen (Denmark), 2007.

[12] Hwang, J.S., Kim, H., Kim, J., “Estimation of the modal mass of a structure with a tuned-mass damper using H-infinity optimal model reduction”, Engineering Structures, 28(1), 2006, pp. 34–42.

[13] Brownjohn, J.M.W., Pavic, A., “Experimental methods for estimating modal mass in footbridges using human-induced dynamic excitation”, Engineering Structures, 29(11), 2007, pp. 2833–2843.

[14] Porras, J.A., De Sebastian, J., Casado, C.M., Lorenzana, A., “Modal mass estimation from output-only data using oscillator assembly”, Mechanical Systems and Signal Processing, 26(1), 2012, pp. 15–23.

[15] Cara, J., “Computing the modal mass from the state space model in combined experimentalâĂŞoperational modal analysis”, Journal of Sound and Vibration, 370, 2016, pp. 94–110.

[16] Reynders, E., Degrauwe, D., De Roeck, G., Magalhães, F., Caetano, E., “Combined Experimental-Operational Modal Testing of Footbridges”, Journal of Engineering Mechanics, 136(6), 2010, pp. 687–696.

[17] Brandt, A., Berardengo, M., Manzoni, S., Cigada, A., “Harmonic scaling of mode shapes for operational modal analysis”, Proceedings of International Conference on Noise and Vibration Engineering (ISMA), September 17-19, Leuven, Belgium, 2016.

[18] Brandt, A., Berardengo, M., Manzoni, S., Cigada, A., “OMAH - operational modal analysis mode shape scaling by means of harmonic forces”, In review.

[19] Brandt, A., Berardengo, M., Manzoni, S., Cigada, A., “Using three–parameter sine fitting for scaling mode shapes with OMAH”, Proceedings of the 7th International Operational Modal Analysis Conference (IOMAC), Ingolstadt, Germany, May 10 – 12, 2017.

[20] Ewins, D.J., Modal Testing: Theory, Practice and Application, Research Studies Press, Baldock, Hertfordshire, England., 2nd ed., 2000.

[21] Maia, N., Silva, J. (Eds.), Theoretical and Experimental Modal Analysis, Research Studies Press, Baldock, Hertforsdhire, England, 2003.